THE JOURNAL OF PHYSICAL CHEMISTRY A

pubs.acs.org/JPCA Article

Steady-State Fluorescence Signatures of Intramolecular Singlet Fission from Stochastic Predictions

Published as part of The Journal of Physical Chemistry virtual special issue "Josef Michl Festschrift".

David J. Walwark, Jr. and John K. Grey*

Cite This: https://dx.doi.org/10.1021/acs.jpca.0c06966 Read Online

ACCESS | Metrics & More | Article Recommendations | Supporting Information

ABSTRACT: The advent of new multichromophoric systems capable of undergoing efficient intramolecular singlet fission (iSF) has greatly expanded the range of possible motifs for multiexciton generation approaches for organic light energy harvesting materials. Transient absorption (TA) spectroscopic probes are typically used to characterize singlet fission processes that may place limitations on sensitivity and time resolution on scales comparable to the full lifespan of spin-forbidden triplets and interactions. Here, we investigate the ability of fluorescence-based spectroscopic probes to detect iSF activity in isolated dyads based on large substituted conjugated acenes (e.g., tetracene and pentacene derivatives). Photophysical models are simulated from several iSF-active dyad systems reported in the literature using a stochastic approach to assess the sensitivity of steady-state fluorescence to the presence of triplet excitons. The results demonstrate large fluctuations in expected fluorescence yields with varying excitation rate constants for systems with $\Phi_{iSF} > 0.5$ (assuming weak interchromophore coupling). Exciton−exciton interactions are also investigated, and we further demonstrate how treating iSF dyads stochastically (i.e., finite number of chromophores) accentuates dependences of photophysical yields with excitation rates. Last, our approach reveals the potential ability of single molecule level fluorescence spectroscopy to detect iSF activity that can aid efforts to design and optimize candidate iSF systems.

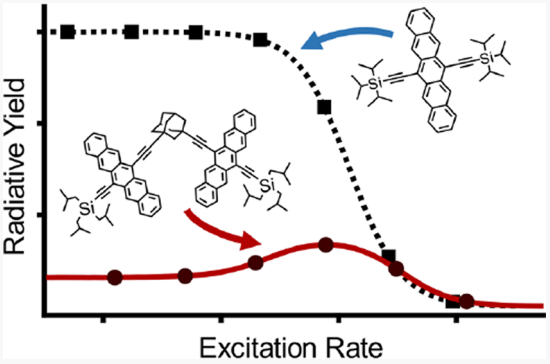

1. INTRODUCTION

Accurate control of singlet fission (SF) yields and effective management of triplet excitons on long time scales (e.g., microseconds to milliseconds) is essential for realizing large performance gains in organic photovoltaic devices.[1] Singlet fission can occur when an excited singlet state on one chromophore delocalizes across a neighboring chromophore and produces an entangled triplet pair state, which may decohere later into independent triplet excitons.[2] At later times, triplet−triplet annihilation (TTA) is possible once triplets separate and is usually undesirable in photovoltaics but essential in other optoelectronic applications, such as upconversion-based systems.[3−5] Both biexcitonic processes often span a broad range of characteristic time scales and must be precisely understood in order to harness the full potential of multiexciton generating systems for photovoltaic applications.

SF was discovered in anthracene crystals in 1963 (intermolecular singlet fission, or, xSF), and subsequent work heavily employed crystals of larger acenes, such as tetracene and pentacene.[6−9] In an essential experiment, Arnold et al. investigated the effect of blocking diffusion of triplet excitons in a tetracene crystal, which sheds light on factors affecting decoherence of triplet pairs and possible fusion (i.e., TTA) at later times.[10] By doping tetracene with varying amounts of 2,3-benzocarbazole, the authors systematically reduced the 2-dimensional diffusion of triplet excitons, forming so-called "exciton cages".[10,11] Within these cages, productive sites for xSF face significantly increased triplet concentrations and increased caging was shown to increase singlet lifetimes from 100 to 360 ps, as well as modify the ratio of emission yield at low versus high intensities. Consequently, the singlet fission rate decreased due to the caging effect suggesting the presence of triplets inhibits singlet fission, consistent with increases in the emission yield and singlet lifetime. Together with stochastic considerations, we further explore the effect of triplets on the efficacies of SF in isolated systems and the ability of fluorescence-based detection to resolve this multi-exciton generating process.

Intramolecular singlet fission (iSF) is a relatively new phenomenon that does not require crystalline solid forms (i.e.,

Received: July 29, 2020
Revised: October 1, 2020

https://dx.doi.org/10.1021/acs.jpca.0c06966
J. Phys. Chem. A XXXX, XXX, XXX−XXX

close-packed chromophores in well-defined orientations) which has spurred intense study for light energy harvesting applications. Though iSF oligomers and polymers may ultimately be preferred for device applications,[12−14] iSF-active dyads are more advantageous for basic studies.[15] Despite the broader palette of iSF materials and greater tunability of molecular architectures and geometries, characterization studies mainly rely on time-resolved absorptive probes at the ensemble level that average over possible conformational states.[12−15] Moreover, current understanding originates largely from single crystalline systems where long-range periodicity makes the effective number of chromophores immense and well-described with deterministic modeling. Juxtaposing these views with iSF materials can be difficult because of fluctuations and variations in molecular geometry and packing at the bulk level. However, recasting iSF as a unimolecular reaction avoids any approximations employing bimolecular formulations (Figure S1).[17,18]

Stochastic methods, on the other hand, offer high fidelity modeling and better capture the molecular-level photophysics of iSF systems where it is more straightforward to handle reactions of higher order. Furthermore, ease of extending models to steady-state illumination, freedom from accumulated numerical error, and flexibility to explore the effect of chromophore number (N_C) are some advantages of stochastic simulations. It is therefore desirable to re-evaluate the pictures of intramolecular biexcitonic reactions in isolated dyads from a completely stochastic perspective, which offers new opportunities for broadening useful physical probes to detect SF activity.[16] It is for these reasons that we seek to re-evaluate intramolecular biexcitonic reactions in isolated iSF dyads from a completely stochastic perspective, which reveals new opportunities for broadening useful physical probes to detect SF activity.

Experimental singlet fission studies (xSF or iSF) have traditionally relied on identifying transient absorption (TA) signatures of triplet pair states (e.g., TT) as the basis for tracking triplet population dynamics, usually on ultrafast time scales.[2,6] However, the operating window of time scales are usually limited due to the relatively short lifetime of TT states whereas decohering and interactions of separated triplets may take place on much slower time scales (e.g., nanoseconds up to microseconds).[2] This large potential gulf in time produces significant experimental challenges for resolving triplet population dynamics over the entire effective range of SF processes. While multiple time-scales can ultimately be studied via more specialized TA experiments, concentrations typically required are high enough to introduce self-interaction effects capable of obscuring the essential intramolecular kinetics.[19] In a similar vein, signal-to-noise limitations of absorptive techniques usually provoke the use of high peak excitation intensities making higher order decay pathways more accessible due to larger exciton densities. Clearly, TA studies of SF would benefit from corroboration via other techniques with higher sensitivity on longer time scales.

Fluorescence spectroscopic probes are among the most sensitive for resolving specific molecular photophysical processes (e.g., charge and energy transfer as well as triplets), thereby enabling study of extremely dilute solutions or solid dispersions using much lower peak excitation intensities than typically employed by TA probes. As we detail below, fluorescence experiments are potentially amenable to study iSF materials since stochastic extrapolation of experimentally derived kinetic schemes predicts pronounced changes in fluorescent signatures due to iSF with excitation conditions. The aim of this paper is 2-fold: to predict new avenues for fluorescent detection of iSF and to highlight the sensitivity of these probes when iSF is treated from a stochastic perspective which supports the viability of single molecule level studies. We perform kinetic Monte Carlo (KMC) simulations of previously published deterministic models of iSF dynamics measured from various dyads based on large acene derivatives (i.e., tetracene and pentacene). We demonstrate that these can be straightforwardly dovetailed into a stochastic framework to extrapolate triplet population dynamics and various quantum yields recorded under steady-state conditions. Because single molecule spectroscopy (SMS) is best suited for resolving stochastic processes experimentally, the predictions herein demonstrate the promise of these techniques to reliably detect iSF activity.

2. METHODOLOGY

2.A. Exploring the Role of Fluorescence Emission in Elucidating Singlet Fission. As an aid to TA experiments, fluorescence studies of SF materials have potential for extending accessible time ranges and sensitivity levels of iSF detection. Time-resolved fluorescence spectroscopy is perhaps most useful for corroborating singlet state lifetimes and repopulation kinetics (i.e., TTA, or, triplet-pair fusion). With the singlet lifetime established via fluorescence decay, TA techniques confirm singlet fission by correlating ground and excited singlet state populations, since SF requires adjacent ground state chromophores to proceed.[2] However, harmonizing results from time-resolved fluorescence and absorptive techniques may experience complications due to differences in peak intensities affecting photophysical pathways and branching ratios.[20,21]

Unlike direct detection of triplet species via absorption-based transitions, fluorescence reporters of triplets are always indirect. However, the higher sensitivity of the fluorophore to its immediate environment better reveals the influence of these and other "dark" excited states. To date, the most distinct and, possibly, direct fluorescence signature of SF is quantum beating in delayed fluorescence decays, a phenomenon only reported in xSF systems.[22−26] This limitation may be due to the homogeneity of triplet state energies in organic crystals that is impossible to recreate in solution-based samples even at exceptionally dilute levels.[27] Other fluorescence techniques that observe magnetic-field effects (MFE) on fluorescence emission may also provide unambiguous evidence of singlet fission (i.e., triplet pair state sublevels), but are likely intractable in single molecules with no well-defined orientational qualities or homogeneity of nanoenvironment.[28,29] Long-time scale delayed fluorescence (with singlet spectral features) remains the sole emissive signature of iSF, though still an indirect reporter.[30] In iSF systems without significant repopulation of the singlet state through triplet fusion (i.e., pentacene-based), most of the aforementioned techniques are not applicable. Even in tetracene-based iSF materials, as molecular design improves and branching ratios change, delayed emission is reduced, rendering experimental techniques reliant upon its detection more prone to noise.

Thus, there are few, if any, known methods to employ fluorescence techniques to identify singlet fission processes and its various products in iSF systems. Under the assumption of weak interchromophore coupling within a dyad construct and

https://dx.doi.org/10.1021/acs.jpca.0c06966
J. Phys. Chem. A XXXX, XXX, XXX−XXX

Table 1. Overview of Model Parameters Used to Calculate Rates and Yields of iSF Monomers and Dyads[a]

System	Absorbing State	Resultant State	$\Phi_r(abs.state)$	Notes
Monomer ($N_C = 1$)	S_0	S_1	k_r/k_s	k_S=k_r + k_{ic} + k_{ISC}
	S_1	S_n	0	Failed absorption or fast internal conversion
	T_1	T_n	0	Failed absorption or fast internal conversion
Dyad ($N_C = 2$)	S_0S_0	S_0S_1	$\frac{k_r + \beta \cdot k_{SF}}{k_s + k_{SF}}$	k_S=k_r + k_{ic} + k_{ISC} ; β is the proportion of singlet fission resulting in emission, $\Phi_{exc}(S_0S_0) \equiv 1$
	S_0T_1	S_1T_1	$\frac{k_r}{k_s + k_{ST}} \cdot \Phi_{exc}(S_0T_1)$	Absorption by ground state with an excitation yield of $\Phi_{exc}(S_0T_1)$= 0.5 to account for ground state bleach; k_{ST} accounts for singlet-triplet annihilation[a]
	S_0S_1	S_1S_1	$\frac{k_r}{k_s + k_{SS}} \cdot \Phi_{exc}(S_0S_1)$	Absorption by ground state, rather than S_1, presumed with an excitation yield of $\Phi_{exc}(S_0S_1)$, which is set to 0.5 to account for ground state bleach; k_{SS} is the singlet-singlet annihilation rate constant[a]
	S_1T_1	S_nT_1	0	Failed absorption or fast internal conversion presumed. Emission only occurs from S_1
	T_1T_1	T_1T_n	0	Failed absorption or fast internal conversion
	TT	TT^*	0	Failed absorption or fast internal conversion

[a]We included the possibility of singlet−singlet and singlet−triplet annihilation (i.e., k_{SS} and k_{ST}, respectively) in the formal definition even if models do not specify these processes.

that the presence of triplets deactivates iSF in a dyad, we demonstrate that varying the photoexcitation rate constant (k_{exc}) can in principle reveal the presence of SF in steady-state fluorescence intensities. We further show that these signatures are most accentuated in dyads by treating iSF from the stochastic viewpoint, suggesting single molecule level probes can in fact detect singlet fission.

2.B. Stochastic Approach to Resolving Singlet Fission from Fluorescence Yields. In our discussion of excitonic states on monomer (e.g., single pentacene or tetracene derivative) and corresponding dyad systems, we use common symbolisms to denote possible configurations. For example, S_0 represents a relaxed monomer (i.e., in its ground electronic state), whereas a singlet exciton on a monomer is represented by S_1. For dyads, we likewise use S_0T_1 to specify a single triplet present, whereas TT represents an entangled pair state with undefined multiplicity. In some cases, TT multiplicity may be included, namely, when applied magnetic fields were used to unambiguously discern these distinct states.

The predictive capabilities of our modeling approach are based on two related assumptions. First, we assume S_1T_1 is a possible excited state of a dyad, which is only valid in systems with weak interchromophoric coupling. Therefore, we presume $S_0T_1 \xrightarrow{k_{exc}} S_1T_1$ is a possible outcome of excitation that is bolstered by the fact that triplets are known to be more localized than singlets. Our second principal assumption is that the presence of a triplet inhibits singlet fission in a S_1T_1 dyad, as suggested from studies of doped crystalline tetracene by Arnold et al.[10]

The simulations also ignore excited state absorption, thus excluding some photophysical processes, such as, reverse intersystem crossing (RSC) from higher triplet states $T_n \rightarrow S_n$, or intersystem crossing (ISC) from higher singlet states $S_n \rightarrow T_n$. While such processes are clearly operative in some cases (e.g., nonsubstituted pentacene with vanishing triplet yields at low temperatures due to deactivation of the $S_1 \rightarrow T_2$ ISC channel),[31] among contemporary iSF literature there are few estimates of the specific kinetic rates. Ignoring excited state absorption by triplets is a good approximation when excitation is on resonance with $S_0 \rightarrow S_1$, but not $T_1 \rightarrow T_n$ (which is experimentally possible in iSF dyads studied herein). If only excited states are present, then they are presumed to either not absorb the exciting photon or absorb it and (instantaneously) vibrationally relax similar to Kasha's rule; both outcomes are considered a "failed absorption" due to our bias toward reactions that change the system state for longer than ∼1 ps. Under low excitation rates, failed absorptions are ≈0 and the quantum yield of excitation is one: Φ_{exc} = 1. This assumption is

https://dx.doi.org/10.1021/acs.jpca.0c06966
J. Phys. Chem. A XXXX, XXX, XXX−XXX

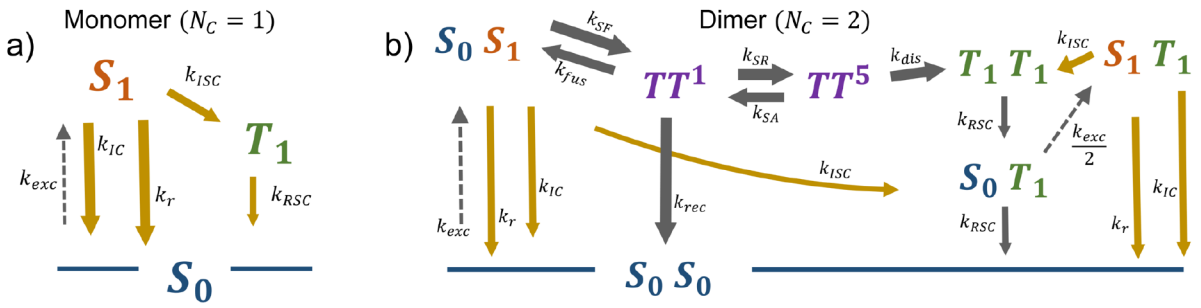

Figure 1. Cartoon diagrams of example monomer (a) and dyad (b) photophysical models. The depicted dyad model is based on the PD-A system from Basel et al.[46] but extended for steady-state simulation. Complete details of all dyad structures and models can be found in the Supporting Information.

implicit in experimental measurements of the fluorescence quantum yield, Φ_r.

We then designed a stochastic simulation algorithm based on the modified next reaction method by Anderson, which is an evolution of the Gibson and Bruck algorithm.[32,33] The flow of the algorithm is as follows: Each reaction channel is given an exponentially distributed resolution-time inversely scaled by the number of reactants and the reaction rate (more reactants and/or a faster rate means less time will elapse before that reaction occurs). Simulation time is advanced to the soonest occurring resolution-time (i.e., next reaction method), the chosen reaction is resolved with discrete stoichiometry, and any newly possible (or, just resolved) reaction is provided a resolution-time before the process repeats. Stochastic simulation of reaction systems is exact and approximation-free, but the technique requires multiple realizations to produce a low-noise average.

Next, the simulated experiment tracks the excitation rate dependence of the state populations and quantum yields of each possible reaction, which is accomplished by simulating 100+ s of time while decreasing the excitation rate constant continuously from its maximum to minimum values (e.g., 10^9 to 10^2 s^{-1}, see Figure S2). During the simulation experiment, the system is constantly relaxing but is never far from total equilibration. Sampling points in time (vertical lines in Figure S2a) are also chosen such that the maximum excitation rate in a time segment is no more than 1% greater than the minimum excitation rate in that same segment.

Excitation times for this experiment are also generated as a nonhomogeneous Poisson process, specifically by a thinning method,[34] which uses an analytic expression and uniform random numbers to check the validity of candidate excitation events generated at the maximum rate. Thus, before the KMC process begins, the excitation times are already determined, and if one relaxed chromophore is present in the system, there is a nonzero probability that absorption will take place. However, we reduce the probability of excitation for these mixed states, such as S_0T_1, and we include the corresponding factor ($\Phi_{exc}(state)$) in each relevant expression presented below in Table 1. For example, we assume that $\Phi_{exc}(S_0T_1) \equiv 50\%$ unless indicated otherwise due to the inability of the triplet to absorb and only one S_0 site available. This procedure is carried out by comparing a uniformly distributed random number between 0 and 1 to the proportion of ground states, with excitation accepted if $random < S_0/N_C$.

Importantly, the excitation of ground-state chromophores is usually not included in deterministic simulations of excited state population dynamics, including experimentally sourced kinetic models used herein (vide infra). For comparison, most TA experiments are modeled as a prepared quantum state that subsequently relaxes after the exciting pulse ends and the prompt excited singlet state probability or, the concentration of the system state (e.g., S_0S_1) is typically normalized to 1. Since we are interested in the effect of varying excitation rates on steady-state populations, it is necessary to go beyond this paradigm. To do so, we modify the adapted models for each dyad system to include the $S_0 \xrightarrow{k_{exc}} S_1$ reaction explicitly.

We also included the possibility of ISC ($S_1 \xrightarrow{k_{ISC}} T_1$), even if the source model did not, which was done to increase realism of steady-state populations. This was accomplished by subtracting the TIPS–pentacene model chromophore ISC rate constant ($k_{ISC} = 1.43 \times 10^6$ s^{-1}) from the singlet decay rate, as well as its radiative rate constant ($k_r = 5.36 \times 10^7$ s^{-1}), which effectively preserved the reported singlet lifetime and fission yields from source models. The remainder of the singlet decay rate can be allocated to nonradiative decay (internal conversion, $S_1 \xrightarrow{k_{IC}} S_0$). For comparison, we consider a tetracene dyad model from Matsui et al.[35] that explicitly included ISC and internal conversion, thus requiring no modifications in our adaptation.

3. RESULTS AND DISCUSSION

3.A. Absorbing States of Single Chromophores. We first consider discrete configurations that collectively describe the kinetic outcomes following absorption of an exciting photon for iSF dyads and a model monomer (e.g., TIPS–pentacene). When correctly defined, these absorbing states dictate the photophysics accessible by experiment. Simulation and experiment can then be connected via the relative probabilities of each of the absorbing states and their emission yields in the steady-state limit, which is our main focus. Absorbing states and their emission yields for a monomer and iSF-active dyad are defined in Figure 1 with detailed descriptions of each term provided in Table 1. We further denote each by their respective number of chromophores, N_C, i.e., monomer, N_C = 1, and dyad, N_C = 2.

Table 1 summarizes in detail the quantum yields of emission for possible absorbing states in both a monomer and dyad system. Within the first three rows that comprise the monomer entries, only one absorbing state has a nonzero emission yield: the ground state S_0. Due to our assumptions that T_n will not relax to a singlet and that relaxation within S_n follows Kasha's rule, when the absorbing state is an excited state (either S_1 or T_1), no emission will follow. While strictly possible, we do not

https://dx.doi.org/10.1021/acs.jpca.0c06966
J. Phys. Chem. A XXXX, XXX, XXX−XXX

consider phosphorescence emission from T_1 because of the low triplet energies that favor efficient nonradiative decay.[19] Before addressing the dyad absorbing states in Table 1, we first consider an example monomer system as a basis for comparison with predictions from the deterministic limit.

A TIPS−pentacene single-chromophore (i.e., monomer) kinetic model was amalgamated from experimental literature, which is based on results in deaerated toluene solution at submillimolar concentrations.[35−39] Figure 2 shows simulated

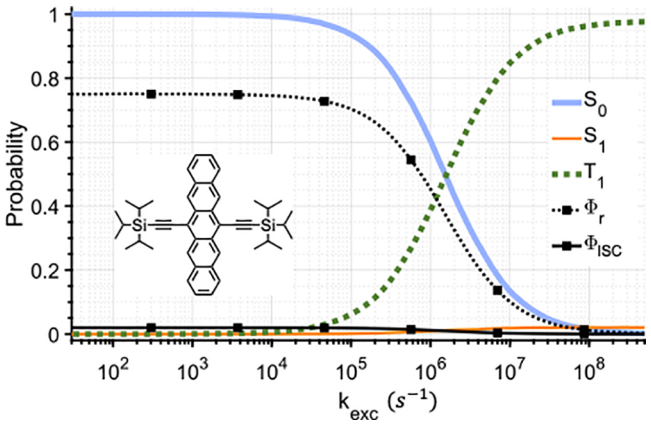

Figure 2. Probability for observing each of the three possible system states in a model pentacene chromophore in addition to radiative and triplet (decay) yields, all as a function of average excitation rate. Note the radiative yield is monotonically decreasing. Key parameters used in this simulation are as follows: τ_{S1} = 14 ns; Φ_r = 0.75; Φ_{ISC} = 0.02; $k_{ISC} = 1.4 \times 10^6\ s^{-1}$; $k_{RSC} = 3.1 \times 10^4\ s^{-1}$; $k_{IC} = 1.6 \times 10^7\ s^{-1}$; $k_r = 5.4 \times 10^7\ s^{-1}$.

probabilities with varying excitation rate constant for a single monomer. The triplet yield of TIPS−pentacene remains controversial, and is markedly affected by the presence of oxygen and self-interaction concentration effects, including xSF.[12,19,40] A value of 0.02 was chosen for $\Phi_{ISC}(S_0)$ which is within reported estimates on large acenes, including oligomers.[29−31,35−40] It is also useful to note that the S_0 absorbing state effectively decides reaction outcomes in this framework, hence, we denote all relevant yields with respect to this state. Our reaction yield results at low excitation intensities match the experimental values of Φ_r and Φ_{ISC} as expected.

Inspecting of Figure 2 from left to right, the excitation rate constant increases (k_{exc}), and the probability of the state S_0 ($\mathrm{Prob}(S_0)$) decreases due to an excited state buildup, i.e., T_1, and to a lesser extent S_1. The singlet yield Φ_{S_1} is the probability of an exciting photon to produce S_1, and it is the same as $\mathrm{Prob}(S_0)$ because the system is a monomer ($N_C = 1$). More generally, at any excitation rate constant, $\Phi_{exc}(k_{exc}) = \mathrm{Prob}(S_0|k_{exc})$, or the yield of the excited singlet state at a given excitation frequency equals the probability of the ground state at that given excitation rate.

Since Φ_{exc} is the yield of relevant excited states (T_n and S_n are not considered here), all the other reaction yields exist within its envelope. That is, $\sum_n \Phi_n = \Phi_{exc}$, where the index n goes over all reactions that have S_1 as a reactant. The emission yield for a monomer at an arbitrary excitation rate is then given by $\Phi_r(k_{exc}) = \Phi_r(S_0)\cdot\Phi_{exc}(k_{exc}) = \Phi_r(S_0)\cdot\mathrm{Prob}(S_0|k_{exc})$. Because monomeric systems have only one absorbing state with nonzero emission yield, their $\Phi_r(k_{exc})$ curves will always be monotonically decreasing due to higher excitation rates depleting ground states. In a similar vein, their fluorescence lifetimes τ_s will remain the same regardless of k_{exc}, since T_1 states cannot contribute to the observed fluorescence decay, which will be considered in a future study.

Due to the lack of bimolecular processes, there is no difference between the stochastic and deterministic results for a monomer system. The case of the monomer was included here to only validate the ability of the model to reproduce the expected photophysics of the canonical three-level system involving a triplet, which also provides a useful basis for comparison when bimolecular processes become accessible in the dyad case. Comparison of Figure 2 and Figure S3 (see Supporting Information), fluorescence intensity saturation occurs at the same excitation rate constant value regardless of the method (i.e., stochastic vs deterministic). Additional examples of deterministic simulations of multiple monomers, including TIPS−pentacene, are also located in the Supporting Information. In the monomer limit, the deterministic results are also approximation-free, which serves as a vital check for the accuracy of our stochastic algorithm. For 3-level single-chromophores, stochastic methods are therefore of limited utility since they exceed the deterministic solutions in providing the variance of probabilities, or exact emission times (e.g., for simulating correlation spectroscopies), but require longer execution times. The exact analytic expressions for steady-state populations ($\mathrm{Prob}(state|k_{exc})$) and relaxation eigenvalues in a 3-level system are provided in the Supporting Information for reference.

Note that for these 3-level systems the sigmoidal shape of the S_0 probability on a semilog plot is persistent, with only the horizontal positioning changing for species ranging from polymers with high triplet yield to small molecule dyes with low triplet yields (Figure S3). This result suggests the $\Phi_r(k_{exc})$ experimental traces can be fit without knowledge of absolute excitation rates and used to extract triplet kinetics or other quantities from steady-state fluorescence, given adequate constraints. While experiments involving saturation or excitation intensity-dependence are often performed using single-molecule fluorescence spectroscopy,[41−43] measuring and modeling $\Phi_r(k_{exc})$ is not a common approach,[44] despite some seminal examples of its utility,[10,29] because of the tacitly assumed linearity of the fluorescence response (triplet−triplet annihilation upconversion systems notwithstanding).

3.B. Absorbing States of Dyads and Fluorescence Emission As a Reporter of Singlet Fission. In contrast to monomers, iSF-active systems formulated in terms of bimolecular reactions may not always be well described by deterministic kinetics. For example, deterministic approaches are most applicable when large reactant numbers are realized or when bimolecular reactions can be reformulated as first-order reactions between system states. Usage of this paradigm for time-resolved experiments is appropriate and has few disadvantages. However, even when bimolecular reactions can be excluded from the reaction rate equations, the extension to steady-state kinetics is convoluted, requiring numerous additional reactions to accurately model the system. For instance, exploring the effect of chromophore number is difficult and error-prone without explicit bimolecular reactions, as a different kinetic scheme and constituent reactions must be formulated for each case. For these reasons, we recast iSF kinetic models in terms of a stochastic framework with bimolecular reactions, which is essential for accurately exploring the ramifications of our primary hypothesis that

https://dx.doi.org/10.1021/acs.jpca.0c06966
J. Phys. Chem. A XXXX, XXX, XXX−XXX

triplets inhibit SF. Scheme 1 illustrates the possible pathways generally available in iSF active dyads that accounts for all possible pathways leading to fluorescence emission.

Scheme 1. Diagram of Photophysical Processes Leading to Fluorescence Emission in iSF Dyads with Dyad States Provided in Table 1

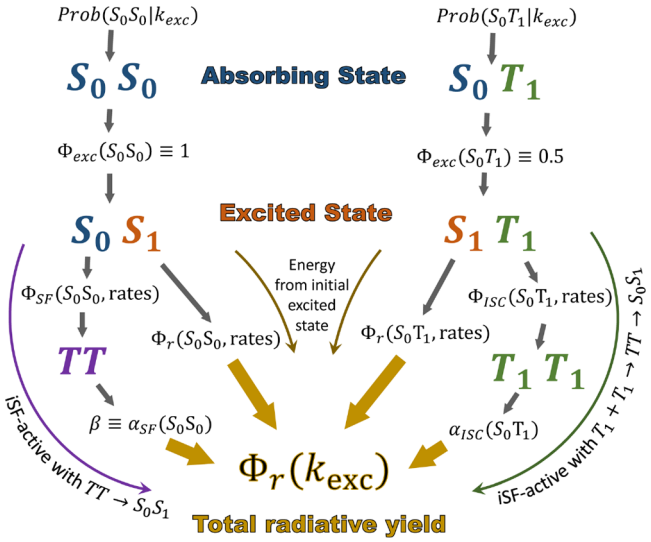

Figure 3 illustrates the structure and predicted populations and reaction yields for an example dyad (i.e., PD-A) with the corresponding states provided in Table 2. Rates of singlet−triplet annihilation ($S_1 + T_1 \xrightarrow{k_{ST}} S_0 + T_1$) and triplet−triplet annihilation ($T_1 + T_1 \xrightarrow{k_{TT}} TT$) are set to zero for this simulation. Because a ground state is required as a reactant, only the S_0S_0 absorbing state possesses a iSF channel. In iSF-active systems, the emission yield is always lower than that of the constituent monomers, even when all the iSF reactions are reversible (i.e., the initial, emissive S_1 state may be recovered). Due to this possibility of reversibility, we introduce a term, β, to detail the proportion of singlet fission reactions (see Scheme 1, vide supra) resulting in fluorescence emission with the yield, $\Phi_r(S_0S_0)$, being $\frac{k_r + \beta \cdot k_{SF}}{k_s + k_{SF}}$, which is the sum of two yields. The first component assumes no singlet reformation following SF where $\Phi_r(S_0S_0, rates) = k_r/(k_S + k_{SF})$ where $k_S = k_r + k_{ic}$. The second component is the SF yield, also assuming no S_1 reformation, $\Phi_{SF}(S_0S_0, rates) = k_{SF}/(k_S + k_{SF})$. We scale $\Phi_{SF}(S_0S_0, rates)$ by β to combine the reversibility effects on emission into one term. The inclusion of "*rates*" within the parentheses means that no stochastic simulation was required to determine the quantity, which is the case for these initial reaction yields. When reversible reactions are not involved, such as in the case of the S_0T_1 state, $\Phi_r(S_0T_1, rates) = \Phi_r(S_0T_1)$, and we forego the "*rates*" designation.

In this work, $\Phi_{SF}(S_0S_0, rates) \neq \Phi_{SF}(S_0S_0)$ because in calculating $\Phi_{SF}(S_0S_0)$ we subtract the number of $TT \rightarrow S_0S_1$ reactions from the number of $S_0S_1 \rightarrow TT$ reactions. Triplet pairs that recombine are also not counted, and this "net SF yield" emphasizes the importance of useful products, i.e., separate triplets. Experiments are usually interpreted under the assumption that $Prob(S_0S_0) = 1$; thus, $\Phi_r(S_0S_0) = \Phi_r(exp)$. This is a good assumption for TA studies using low repetition-rates (time between pulses $>5\tau_{triplet}$), or for emission yields

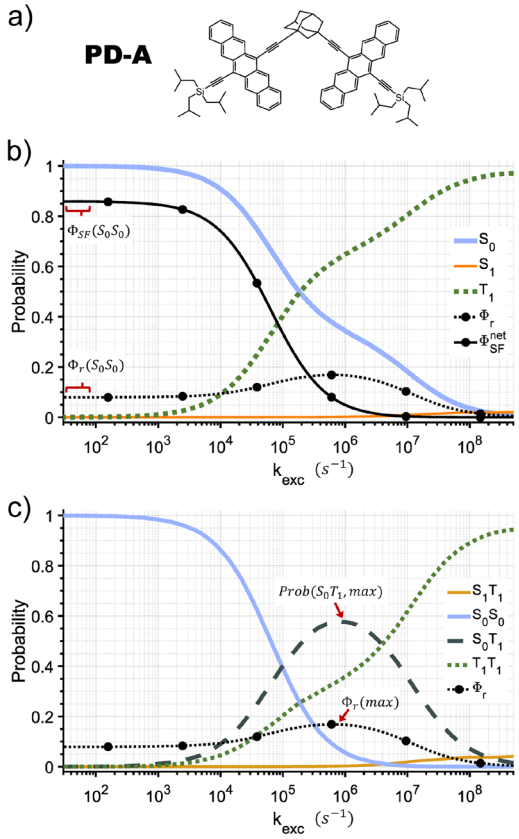

Figure 3. (a) Sketch of PD-A (adapted from ref 46.). (b) Chromophore-focused populations, radiative, and net singlet-fission yields in PD-A. (c) System-focused populations and radiative yield in PD-A.

performed with low-intensity illumination. Simulation results for low k_{exc} (left-hand side of Figure 3) correspond to $Prob(S_0S_0) \approx 1$, while yields of various reactions in this regime are presented in Table 2 for six different iSF active compounds reported previously in the literature. If the $Prob(S_0S_0) < 1$, measurements on the system may return different results for emission yields and lifetimes, oftentimes in a surprising manner.

In Figure 3b, the probability of the chromophore species (S_0, S_1, T_1) is plotted, not the system state. At the scale of this graph, plotting the pair state TT probability is not useful, as it is approximately zero throughout. This form of visualization is helpful for viewing the total excitation envelope, since, due to our implementation of ground state bleach affecting excitation, $Prob(S_0|k_{exc})$ is exactly the same as $\Phi_{exc}(k_{exc})$, similar to the monomer case. Likewise, we can see that $Prob(T_1)$ increases with k_{exc}, but the disadvantage of plotting the chromophore species is that we cannot use the concept of absorbing states to explain the results. For instance, why does $\Phi_r(k_{exc})$ have a maximum at $k_{exc} \approx 7 \times 10^5$ s^{-1}?

It is a unique advantage of stochastic simulation that the probability of any arbitrary system state can be measured and plotted without resorting to defining each state as an artificial species. Figure 3c plots the absorbing state probabilities revealing that both $Prob(S_0T_1)$ and $Prob(T_1T_1)$ increase as excitation rate increases (middle and right-hand side). Due to their longer (i.e., microsecond) lifetimes, S_0T_1 and T_1T_1 are the most probable and influential states on the fluorescence

https://dx.doi.org/10.1021/acs.jpca.0c06966
J. Phys. Chem. A XXXX, XXX, XXX−XXX

Table 2. Definitions of Photophysical Yields and Model iSF Dyads (See Supporting Information for Corresponding Structures)

system	$\Phi_r(exp)$ (%)	$\Phi_r(S_0S_0, rates)$ (%)	$\Phi_r(S_0S_0)$ (%)	$\Phi_r(S_0T_1, rates)$ (%)	$\Phi_{SF}(S_0S_0, rates)$ (%)	β (%)	$\Phi_{SF}(S_0S_0)$ (%)	$\Phi_{RSC}(S_0S_0)$ (%)
PD-A[a]	1.7	2.15	7.95	56.39	96.19	6.0	85.86	64.46
TD-A[b]	26	26.58	36.58	72.41	63.29	15.8	49.44	10.30
PD-B[c]	–	2.47	2.49	82.42	97.00	0	96.93	108.40
PD-C[d]	–	0.045	0.048	82.42	99.95	0	99.93	20.28
PD-D[e]	3.5	16.23	17.12	28.19	42.42	2.1	39.26	42.65
PD-E[f]	9.9	26.79	27.14	35.71	25.00	1.4	24.02	21.66

[a]"NC" in source.[46] Model includes two pair states of different multiplicity and extensive reversible reactions. Featured in Figure 3. [b]"Tc-Ad-Tc" in source. TIPS−tetracene based. Model has one pair state with reversible pathway to separated triplets; the only model with triplet−triplet annihilation.[38] [c]"Meta" in source. Model has one pair state and no reversible reactions.[37] [d]"Ortho" in source. Model has one pair state and no reversible reactions.[37] [e]"C" in source. Model identical with PD-A with addition of singlet solvent relaxation.[47] [f]"D" in source. Model identical with PD-A with addition of singlet solvent relaxation.[47]

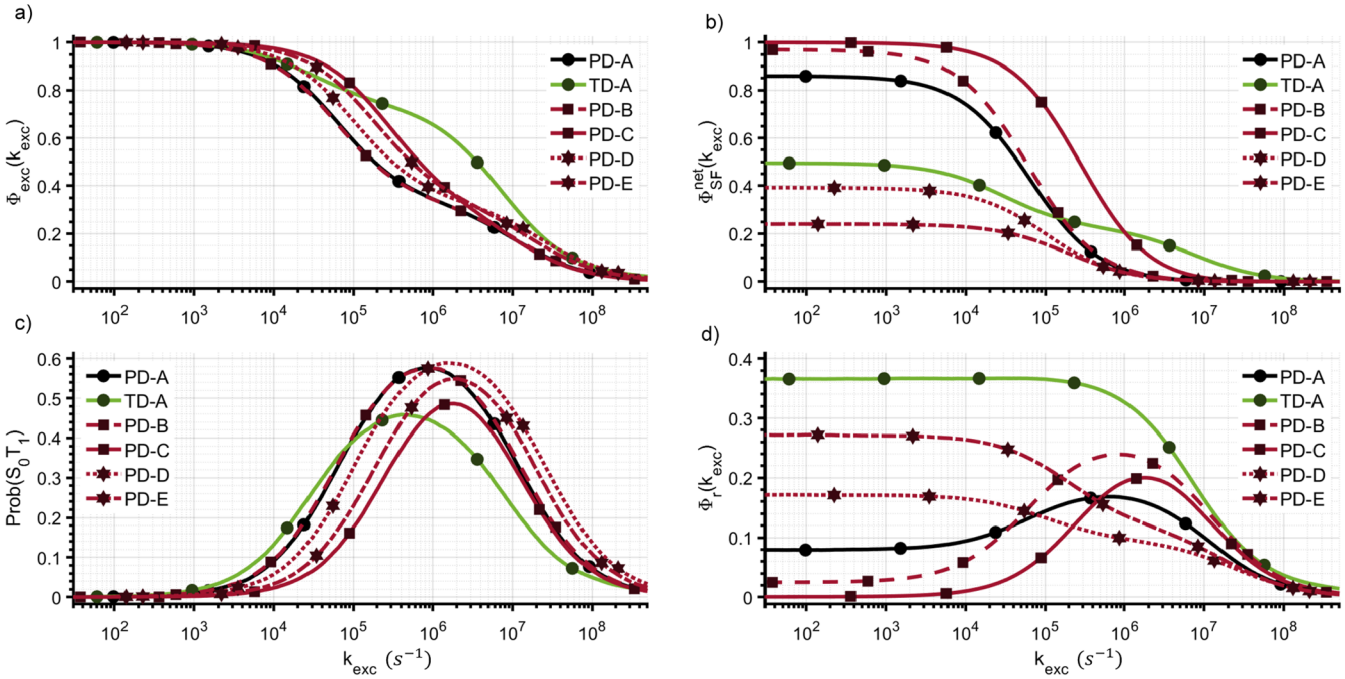

Figure 4. Excitation intensity dependent excitation yields, $\Phi_{exc}(k_{exc})$ (a), net singlet fission yield, $\Phi_{SF}(k_{exc})$ (b), S_0T_1 probabilities (c), and radiative yield, $\Phi_r(k_{exc})$ (d), for all model iSF systems.

outcomes besides S_0S_0. Explicitly, the radiative yield in a dyad is a probability weighted sum of all the emission yields:

$$\Phi_r(k_{exc}) = \Phi_r(S_0S_0)\cdot \mathrm{Prob}(S_0S_0|k_{exc}) + \Phi_r(S_0T_1)\cdot \mathrm{Prob}(S_0T_1|k_{exc}) \quad (1)$$

Thus, unlike the monotonically decreasing $\Phi_r(k_{exc})$ curve from the monomer case, the $\Phi_r(k_{exc})$ curve for a productive iSF dyad will have a peak at intermediate k_{exc} values before succumbing to saturation from high Prob(T_1T_1) or other absorbing states with negligible emission yields at large k_{exc}. We propose that a substantial peak in the $\Phi_r(k_{exc})$ curve is unlikely to be present without efficient singlet fission, although the absence of the $\Phi_r(k_{exc})$ peak should not be taken as proof against the existence of iSF. In general, iSF causes $\Phi_r(k_{exc})$ to take on a more structured appearance than the smooth sigmoidal shape of the monomer on a semilog plot. There is a possibility that other species could impact singlet fission, such as charges, which are probably a bigger factor at higher concentrations. The likelihood of charged species is very low in the case of a single dyad in addition to the fact that singlet fission efficacies are usually much larger as confirmed from TA experiments. Along similar lines, it is interesting to note that our predictions indicate a lower expected $\Phi_{SF}(k_{exc})$ value (see Figure 3b) when iSF dyads are exposed to light intensities similar to AM1.5 conditions (ca. 10^6 s^{-1} based on the approximate area of an iSF dyad) than at lower levels. This effect can be explained in terms of expectations for Prob(S_0T_1) which reach a maximum around the same conditions thereby inhibiting singlet fission.

3.C. Comparisons between Dyad Systems with a Large Range of Reported iSF Yields. We now extend our consideration to six different iSF-dyad model systems with varying iSF yields as reported from TA studies (see Table 2 for labeling assignments and associated parameter values for each dyad).[37,45,47,48] Molecular structures of each dyad and complete rates and reaction schemes may be found in the Supporting Information, which are based on published unimolecular deterministic models. Briefly, we source models for pentacene dyads (PD) and a tetracene dyad (TD), which

https://dx.doi.org/10.1021/acs.jpca.0c06966
J. Phys. Chem. A XXXX, XXX, XXX−XXX

are further designated with a letter as shown in Table 2 (i.e., PD-A). Figure 4 displays simulation results for these systems using our stochastic approach. Despite standardizing all pentacene dyad radiative and ISC rates, predicted $\Phi_r(S_0S_0)$ values are higher than experimental values (left-hand side of Figure 4). Specifically, except for TD-A, all source models neglected to differentiate between singlet decay channels, instead providing a single rate constant for non-iSF decay. We subtracted reported values for radiative emission and ISC from this rate where the remainder was assumed to represent internal conversion. This modification reduces the emission yield, which has greater intuitive appeal than assuming all singlet decay rates are purely radiative. Despite that our modifications exactly preserve the experimentally measured iSF yield resulting in concomitant reductions of the radiative emission yield, our simulated emission yields are still found to be higher than the reported experimental results. For example, PD-A is found to have $\Phi_r(S_0S_0)$ = 7.95%, with the experimental value in benzonitrile provided as $\Phi_r(exp)$ = 1.7% .[45] Many authors ensured good correspondence between $\Phi_r(exp)$ and $\Phi_r(S_0S_0, rates)$, which is akin to ignoring the reformation of emissive singlet states from triplet pairs, a reaction included in all models here except PD-B/C. This apparent shortcoming is understandable since with basic deterministic methods, there is no way to reconcile the kinetic model generated from time-resolved experiments with the steady-state emission yield. If comparing reaction yields from a particular model using a single excitation rate is desired, this may be accomplished straightforwardly using the Cain software package.[49]

In Figure 4a, the excitation yield as a function of excitation rate constant is plotted ($\Phi_{exc}(k_{exc})$). As before, $\Phi_{exc}(k_{exc})$ = Prob(S_0), since excitation relies only on the number of available ground states. This means that any system state with an S_0 constituent underlies the $\Phi_{exc}(k_{exc})$ curve. Explicitly, using the absorbing state probabilities for dyads

$$\Phi_{exc}(k_{exc}) = \mathrm{Prob}(S_0) = \mathrm{Prob}(S_0S_0) + {}^1/_2\cdot\mathrm{Prob}(S_0T_1) + {}^1/_2\cdot\mathrm{Prob}(S_0S_1) \quad (2)$$

where we have again assumed a reduction of absorption cross section by a factor of $^1/_2$. Due to the short-lived nature of the singlet state with an available iSF channel, Prob(S_0S_1) is negligible under most circumstances. The shape of $\Phi_{exc}(k_{exc})$ is made nonsigmoidal by the presence of multiple system states with different excitation probabilities. The similarity of all the systems on this plot is evidence of this fact. If only S_0S_0 absorbs, $\Phi_{exc}(k_{exc})$ would be sigmoidal like the Prob(S_0) for the monomer in Figure 2. TD-A resists saturation because $T_1 + T_1 \xrightarrow{k_{TT}} TT$ is a possible reaction in its original model. In contrast, PD-A and PD-B begin to saturate before all other systems due to their high yields of long-lived triplets (64% and 108% respectively) and lack of a TTA reaction (a typical assumption for models of pentacene-based systems). Figure 4b shows the yield of singlet fission that does not result in a reformed singlet. The variation in $\Phi_{SF}(S_0S_0)$ among the model systems is extensive (see Table 2). The sigmoidal shape of the pentacene dyad systems on this plot arise from two factors: (1) only one absorbing state can perform iSF; (2) lack of a triplet−triplet annihilation channel means there is little correlation between Prob(S_0S_0) and Prob(S_0T_1). In TD-A, Prob(S_0S_0) and Prob(S_0T_1) are highly correlated because a reaction path exists between the states (efficient ISC followed by TTA), thus its $\Phi_{SF}(k_{exc})$ behavior is nonsigmoidal.

To further highlight the observed connection between Prob(S_0T_1) and $\Phi_r(k_{exc})$, Figure 4c plots Prob(S_0T_1) for all the systems. The similarity between all the systems is striking and shows how average excitation rates affects the system state. We can see that the contribution of Prob(S_0T_1) explains only part of the behavior of $\Phi_r(k_{exc})$, since the state-specific emission yields (Tables 1 and 2) are needed. Figure 4d shows the absolute emission yield, and by comparing with Figure 4b, we can see that the correlation between net singlet fission yields and the emission yield peak is clear. PD-A, PD-B, and PD-C all have $\Phi_{SF}(S_0S_0) > 0.8$ and all show a substantial increase in $\Phi_r(k_{exc})$ as k_{exc} approaches 10^6 s^{-1}. TD-A exhibits a miniscule increase in emissive yield: $\Phi_r(max) - \Phi_r(S_0S_0)$ = 0.1% which is imperceptible and, consequently, results in a mostly sigmoidal $\Phi_r(k_{exc})$ curve. PD-D/E have $\Phi_{SF}(S_0S_0) < 0.4$ and deactivating iSF because a chromophore site resides in a triplet cannot make up for the loss of absorption in S_0T_1. These curves also display monotonically decreasing $\Phi_r(k_{exc})$ behavior with nonsigmoidal character (i.e., multiple inflection points) indicating the changing proportions of the photophysically distinct absorbing states. While the effects of iSF on $\Phi_r(k_{exc})$ are varied, systems that efficiently undergo irreversible singlet fission are identifiable by visible contrast in emission quantum yields with increasing excitation rate constant values.

Since we assume an average ground state bleach effect $\Phi_{exc}(S_0T_1)$ = 0.5, the kinetic requirements predicting the existence of an increasing $\Phi_r(k_{exc})$ can be postulated: $2\cdot\Phi_r(S_0S_0) \lesssim \Phi_r(S_0T_1)$, that is, the radiative yield of S_0T_1 must be approximately two times greater than the radiative yield of S_0S_0. TD-A provides a good testbed because its $\Phi_r(k_{exc})$ increases by 0.1% (clearly discernible as a real change despite stochastic noise). The results demonstrate this expression is approximate: $\Phi_r(S_0T_1)/\Phi_r(S_0S_0)$ = 1.98, yet $\Phi_r(k_{exc})$ still increases slightly. If more precision is required, then we should use the exact expression for the condition of an anomalous $\Phi_r(k_{exc})$:

$$\Phi_r(S_0S_0) < \Phi_r(S_0T_1)\cdot\mathrm{Prob}(S_0T_1|k_{exc})\cdot\Phi_{exc}(S_0T_1) + \Phi_r(S_0S_0)\cdot\mathrm{Prob}(S_0S_0|k_{exc}) \quad (3)$$

assuming no emission from other absorbing states besides S_0T_1 and S_0S_0. Importantly, the probability of a particular system state at a given excitation rate is only retrievable from a bimolecular kinetic model with stochastic simulation, which is a complex result of the kinetic scheme and governing rates.

It is also useful to point out that the connection between long-lived triplet yields and emission yield is subtle. By measuring the yield of triplet decay from RSC ($\Phi_{RSC}(S_0S_0)$), we include triplets from all source reactions (i.e., SF and ISC), while excluding those that annihilate, see Table 2. PD-C, which has the largest relative change in its emission yield curve (Figure 4d), only produces 0.2 triplets per excitation. Yet, PD-E, which produces 0.21 triplets per excitation, has no discernible $\Phi_r(k_{exc})$ peak, but only an extra inflection point on its downward path with increasing k_{exc}. Clearly, the main factors in the Prob(S_0T_1) are the overall triplet yield and their decay rate. However, it is apparent in Figure 4c that Prob(S_0T_1), while prone to a slightly displaced location and distribution width, always has a maximum value between 0.45 and 0.6 for the systems modeled here. Thus the most important factor in the shape of $\Phi_r(k_{exc})$ is the ratio of

https://dx.doi.org/10.1021/acs.jpca.0c06966
J. Phys. Chem. A XXXX, XXX, XXX−XXX

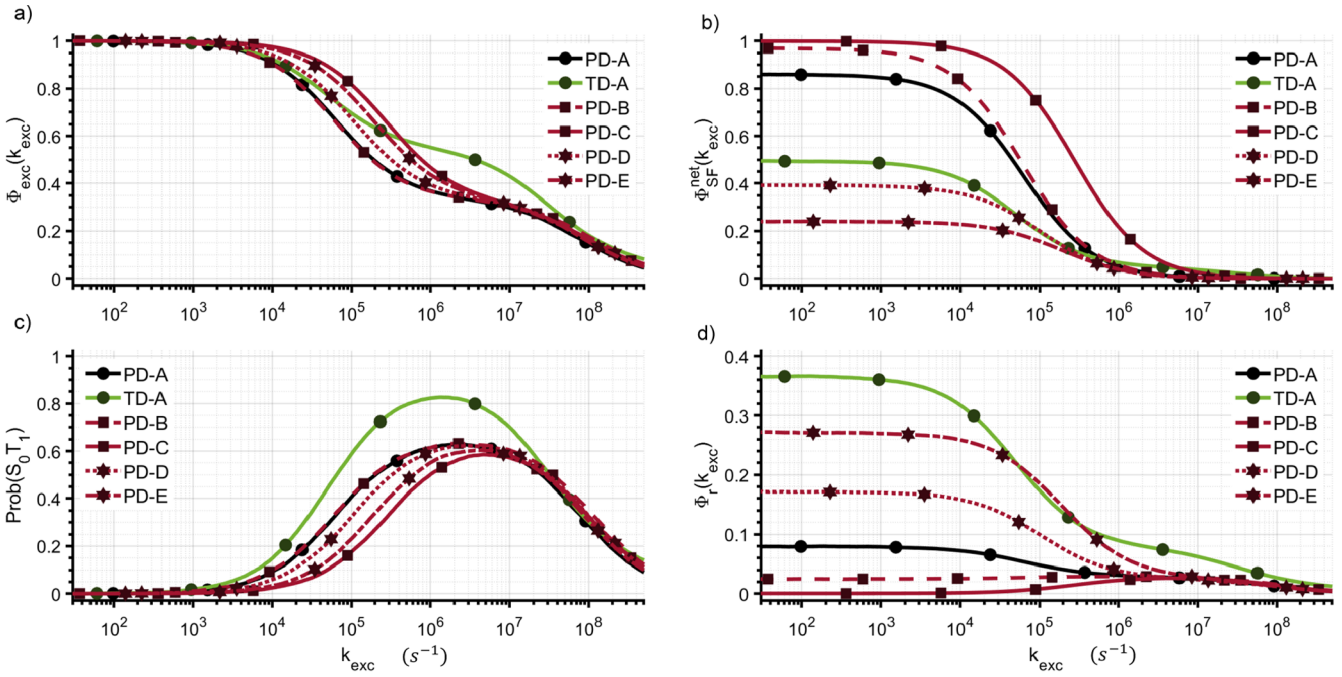

Figure 5. Excitation intensity dependent excitation yields with STA ($k_{ST} = 10k_r$), $\Phi_{exc}(k_{exc})$ (a), net singlet fission yield, $\Phi_{SF}(k_{exc})$ (b), S_0T_1 probabilities (c), and radiative yield, $\Phi_r(k_{exc})$ (d), for all model iSF systems.

emission yields for the most influential absorbing states, S_0T_1 and S_0S_0. For instance, this ratio, $\Phi_r(S_0T_1)/\Phi_r(S_0S_0)$, is 1728 for PD-C, whereas it is 1.3 for PD-E compared to a value of 2 as predicted for an increase in $\Phi_r(k_{exc})$ due to triplet-induced deactivation of iSF. This result explains why PD-C has a pronounced peak in $\Phi_r(k_{exc})$ while PD-E does not. In PD-A, which has an obvious but, relatively modest peak in $\Phi_r(k_{exc})$, the increase in emission is $\Phi_r(max)/\Phi_r(S_0S_0) \approx 2$, and the ratio of the state emission yields is $\Phi_r(S_0T_1)/\Phi_r(S_0S_0) = 7.1$.

3.D. On β and the General Form of $\Phi_r(k_{exc})$. It is now useful to examine the regime of low excitation rates to examine the possibility of reversibility for iSF emission using the reformed singlet emission factor, β, in the following expression:

$$\Phi_r(S_0S_0) = \Phi_{SF}(S_0S_0, rates)\cdot\beta + \Phi_r(S_0S_0, rates) \quad (4)$$

where all terms are given in Table 2 for the six model systems. The PD-B and PD-C systems do not include a singlet reformation reaction, thus their β values are zero. Furthermore, $\Phi_r(exp)$ was not reported, which precludes comparisons to determine whether this assumption is valid. In PD-B/C, any difference between $\Phi_{SF}(S_0S_0, rates)$ and $\Phi_{SF}(S_0S_0)$ or $\Phi_r(S_0S_0, rates)$ and $\Phi_r(S_0S_0)$ is due to stochastic noise indicating a relative error of <1%. If we assume that β is the probability of reforming the singlet state from the triplet pair (i.e., $\Phi_{fus}(TT)$) multiplied by $\Phi_r(S_0S_0, rates)$, we reach an interesting conclusion, namely, the reformation yield is greater than 1. Expanding eq 4 with this assumption,

$$\Phi_r(S_0S_0) = \Phi_{SF}(S_0S_0, rates)\cdot\Phi_{fus}(TT)\cdot\Phi_r(S_0S_0, rates) + \Phi_r(S_0S_0, rates) \quad (5)$$

and solving for $\Phi_{fus}(TT)$,we produce an estimate for $\Phi_{fus}(TT)$ of 280%, using values for PD-A from Table 2. At first, probability estimates greater than 100% appear to be erroneous, however, since the model allows multiple fission and fusion reactions, it can be interpreted as the number of times S_0S_1 is reformed, on average. From this perspective, S_0S_1 emits with a probability, $\Phi_r(S_0S_0, rates)$, each occasion it is reformed. Taking $\alpha_p(state)$ as the terminal emission yield of some reaction p from a system in a given state ($\alpha_p(state)$ is the analog of β, since it is essentially $\alpha_{SF}(S_0S_0)$), we can write the general form of the emission yield as a function of excitation rate:

$$\Phi_r(k_{exc}) = \sum_{states}\sum_{rxns}\Phi_p(state, rates)\cdot\alpha_p(state)\cdot\mathrm{Prob}(state)\cdot\Phi_{exc}(state) \quad (6)$$

In seeking a more comprehensive example, we apply this expression to the TD-A system, since triplet pair-state reformation from separate triplets is energetically accessible in tetracene-based systems. Now, using $\Phi_{exc}(S_0S_0) = 1$ and $\alpha_r(S_0S_0) = 1$,

$$\Phi_r(k_{exc}) = \Phi_r(S_0S_0, rates)\cdot 1\cdot\mathrm{Prob}(S_0S_0)\cdot 1 + \Phi_{SF}(S_0S_0, rates)\cdot\beta\cdot\mathrm{Prob}(S_0S_0))$$

$$\Phi_{ISC}(S_0T_1, rates)\cdot\alpha_{ISC}(S_0T_1)\cdot\mathrm{Prob}(S_0T_1)\cdot\Phi_{exc}(S_0T_1) + \Phi_r(S_0T_1, rates)\cdot 1\cdot\mathrm{Prob}(S_0T_1)\cdot\Phi_{exc}(S_0T_1) \quad (7)$$

where $\alpha_{ISC}(S_0T_1)$ is the terminal yield of emission from creating T_1T_1 from S_0T_1 by ISC, which was visualized in Scheme 1 earlier. In summary, we show that it is possible to account for the probability of return to a state with emission yield from any reaction with that channel available. In this case, the total emission yield is the sum of all those reaction yields multiplied by the probabilities of their precursor states and respective excitation probabilities.

3.E. Effect of Singlet−Triplet Annihilation on Singlet Fission Yields. Because long-lived triplets may quench excited singlets, it is instructive to consider if this anomalous $\Phi_r(k_{exc})$

https://dx.doi.org/10.1021/acs.jpca.0c06966
J. Phys. Chem. A XXXX, XXX, XXX−XXX

phenomenon persists when efficient singlet−triplet annihilation (STA) is operative. STA is typically described in terms of a first order, dipole−dipole coupling (Forster-type) energy transfer mechanism and thereby follows a first order rate constant, k_{ST}, containing appropriate dipole orientation and spectral overlap factors. The STA reaction is given by, $S_1 + T_1 \rightarrow S_0 + T_n \rightarrow S_0 + T_1$, which assumes internal conversion from T_n to T_1 is rapid. Current understanding of possible contributions of STA activity in iSF systems is mostly unknown. It also remains to be seen whether the breakdown of the point dipole approximation necessitates revisiting alternative mechanisms in iSF materials, and to this end, we make no attempt to estimate or use literature precedent for k_{ST}. Furthermore, no accommodation is made to the other rates in the models since there are no relationships to conserve, as there was in the case of our inclusion of ISC under the constraint of preserving the S_0S_0 lifetimes and fission yields. Instead, we explore the effects of STA in a few hypothetical regimes, to serve as a guide for assessing qualitative impact on experiment.

Simulations were performed using a singlet−triplet annihilation rate constant 10 times the radiative rate ($k_{ST} = 10k_r$) that are shown in Figure 5. While $\Phi_{exc}(k_{exc})$ and $\Phi_{SF}(k_{exc})$ (Figure 5, parts a and b, respectively) follow overall similar behaviors as seen in Figure 4, we observe large changes in both Prob(S_0T_1) and $\Phi_r(k_{exc})$ (Figure 5, parts c and d, respectively) for PD systems when STA is nonzero. In particular, the characteristic peak in $\Phi_r(k_{exc})$ has been lost for PD-A (Figure 5d), and strongly reduced in PD-B and PD-C. TD-A, like PD-D and PD-E, also exhibits nonsigmoidal character with apparent multiple inflection points occurring along the $\Phi_r(k_{exc})$ curves. Interestingly, monotonic decreases are observed for all three of these systems. If the existence of triplets deactivates singlet fission while also shortening the singlet lifetime, then there is less possibility for the emission quantum yield to increase. In fact, in Figure 5c we can see that the maximum of Prob(S_0T_1) shifts to larger values of k_{exc} for all systems, and especially for TD-A, demonstrating that a strong reduction in $\Phi_r(S_0T_1)$ is most responsible for the changed shape of the $\Phi_r(k_{exc})$ curves. The large increase of Prob(S_0T_1) in TD-A is due to a decrease in TTA, since TTA creates a pair state from S_0T_1 that can either decay directly to S_0S_0, or repopulate S_0S_1; STA at this magnitude reduces the possibility for S_0T_1 to become T_1T_1 by rendering ISC noncompetitive.

If $k_{ST} = k_{SF}$, then $\Phi_r(S_0T_1) \leq \Phi_r(S_0S_0)$, so $\Phi_r(k_{exc})$ will be monotonically decreasing. In this special case there would be no change in the singlet lifetime at different excitation rate constants. If $k_{ST} > k_{SF}$, then singlet lifetimes would decrease at higher excitation rates, and the system would be more resistant to complete saturation (compare Figure 4a for examples of STA-induced reductions of state probabilities with zero absorption).

3.F. Effect of Chromophore Number. Thus far, simulation results were generated for only two chromophores (i.e., single dyad iSF molecules), which exhibit demonstrably large fluctuations in expected fluorescence emission yields under a varying k_{exc}. We now consider the scenario of approaching the deterministic limit by simply increasing the number of simulated chromophores, N_C. Since a completely deterministic solution implicitly assumes an infinite number of chromophores, we know that using a finite number of chromophores in a stochastic simulation will differ fundamentally from the deterministic solution. The goal here is not to reproduce a deterministic solution exactly but to show the effect of increasing N_C on photophysical products that may be validated later for other multichromophoric iSF systems.

First, it must be noted that, in the framework of our model, the effective rate at which a reaction occurs (i.e., its "propensity") is proportional to the number of reactants. One convenient aspect of iSF dyads is that the propensity for a SF rate that was fit as first order (for instance by creating the "species" S_0S_1) is identical with the bimolecular stochastic propensity. This condition, which preserves the singlet lifetime between deterministic and stochastic modeling, is no longer true when $N_C > 2$. For instance, for the SF reaction: $propensity(SF) = k_{SF} \cdot S_0 \cdot S_1$. In going from two chromophores to three we have doubled the propensity, which is in accord with standard mass action kinetics of bimolecular reactions.[16] On the basis of arguments for entropic contributions to singlet fission, this increase in iSF yield with more chromophores is also consistent with expectations.[50] Moreover, experimental evidence also exists from poly pentacene derivatives in which the internal chromophores (i.e., two nearest neighbors) contribute more to singlet fission than the external chromophores that only have one neighbor.[51] Singlet fission is the only reaction in our simulations to increase in propensity due to an increase in accessible ground states.

In Figure 6, the effect of increasing N_C on species probabilities Φ_{SF} and Φ_r is demonstrated. We have chosen N_C = 2, 3, 4, 6, 10, and 20 for the PD-A system and note that since the x-axis is excitation rate constant, not excitation intensity, N_C merely affects the granularity of the ground state bleach and not the absorptive cross section. In Figure 6a, we see that despite the increase in SF propensity, ground states are more probable in the $k_{exc} = 10^4-10^5$ s^{-1} range. This is simply because when $N_C > 2$, SF no longer depletes all the ground states upon resolution. Furthermore, the stoichiometry is unchanged, despite the presence of more reactants. The complementary behavior is observed in the T_1 probability. To understand what the effect of N_C is in the $k_{exc} = 10^6-10^7$ s^{-1} range, it is important to recall that S_0T_1 is assumed iSF incapable. For example, if instead we have the $S_0S_0T_1$ (i.e., $N_C = 3$) absorbing state, the SF propensity is reduced by the presence of a triplet, but it is not zero. The same can be said in the case of $S_0S_0S_0T_1T_1T_1$ (i.e., $N_C = 6$) where SF yields are reduced but still possible. This approach offers useful intuitive value for understanding predictions from the limit of large N_C, such as, a polymer. In a dyad, the presence of one exciton is highly influential upon its neighboring chromophore, but as we increase the number of chromophores in the system, one exciton is no longer as important. We again reiterate that this rationale only strictly applies in the limit of weak interchromophore coupling, which may not always be the case in some iSF systems, such as, oligomers, and the assumption of mass-action kinetics is implicit as well. The S_0 and T_1 species probabilities also go from moderately structured when $N_C = 2$ to smooth and sigmoidal when $N_C = 20$. In general, larger numbers of chromophores translates into all of the possible absorbing states merging into one inhomogeneously broadened curve.

It is noteworthy that increasing N_C causes $\Phi_{SF}(k_{exc})$ to shift gradually to larger k_{exc} values as expected from mass action kinetics. This behavior simply reflects the existence of more absorbing states capable of undergoing iSF. Figure 6c shows that the $\Phi_r(k_{exc})$ curve becomes invariant at higher decades of excitation rates as N_C increases. In complementary fashion with

https://dx.doi.org/10.1021/acs.jpca.0c06966
J. Phys. Chem. A XXXX, XXX, XXX−XXX

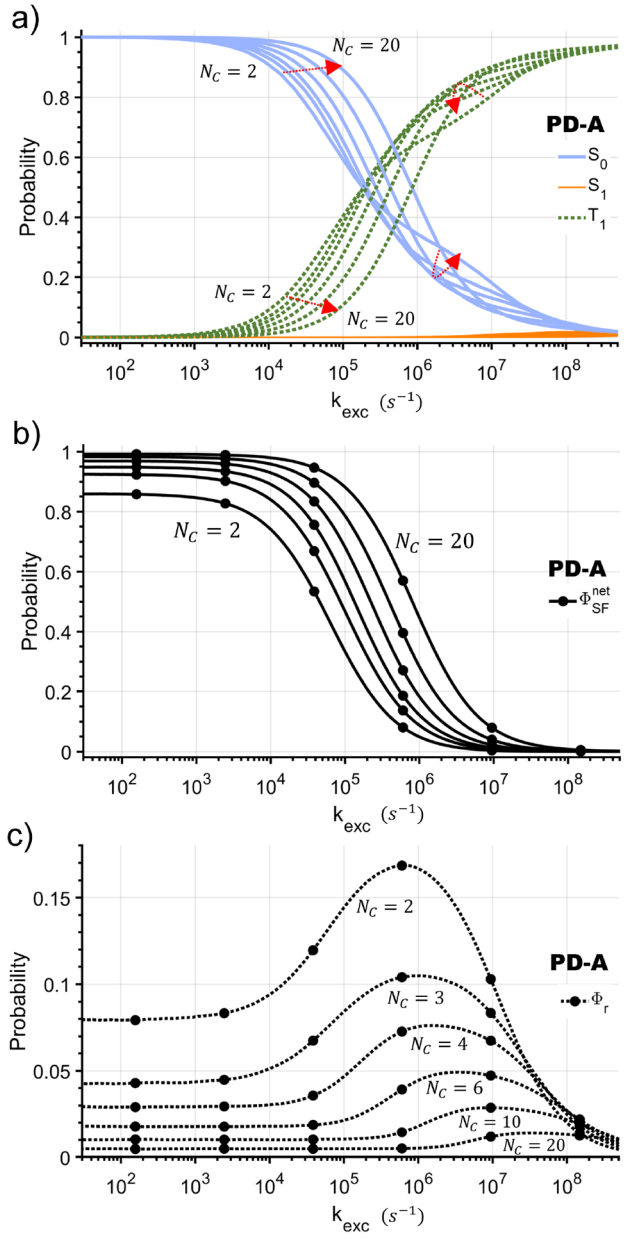

Figure 6. Effect of N_C with excitation rate on (a) state probabilities, (b) $\Phi_{SF}(k_{exc})$, and (c) $\Phi_r(k_{exc})$. Beginning from our initial value (N_C = 2), we increase N_C up to 20 using the PD-A system as a reference.

$\Phi_{SF}(k_{exc})$, $\Phi_r(k_{exc})$ decreases everywhere. Interestingly, the relationship $\Phi_r(max)/\Phi_r(S_0S_0) \approx 2$ is approximately maintained, but the location of $\Phi_r(max)$ shifts to larger values of k_{exc} with increasing N_C.

The results in Figure 6 highlight two key points related to the practical implications of the stochastic kinetic model framework. The first and most important pertains to the transition to the deterministic limit on the predicted fluctuations of the excitation rate dependent steady-state fluorescence yields due to singlet fission. The trends presented herein demonstrate that increasing the number of "virtual" chromophores leads to a reduction in accuracy for a system with only two actual chromophores, when iSF is formulated as a bimolecular reaction. This consideration also represents an important distinction between xSF and iSF where the former possesses a much larger set of intrinsic chromophores whereas the latter is always limited by the constituent chromophores of the chemical structure. Second, steadily increasing realistic numbers of interacting chromophores, such as N_C = 3, 4, and 6, offers novel qualitative views of the possible outcomes for hypothetical iSF systems in addition to illuminating the border of deterministic applicability.

4. CONCLUSIONS

We have demonstrated large fluctuations and multiple inflection points in excitation rate dependent steady-state fluorescence yields of iSF-active dyad molecules. By simulating existing photophysical models stochastically, we have shown the ability of fluorescence-based probes in general to detect singlet fission processes for iSF-active systems. In particular, dyads with high net singlet fission yields show anomalous behaviors in $\Phi_r(k_{exc})$ responses, where the emission yield increases with increasing excitation rate constant, due to the presence of triplets. Assuming mass-action kinetics hold, a similar signature is predicted to exist for larger oligomers as well. While this study concentrated on dyads containing pentacene derivatives, similar results have been demonstrated in tetracene crystals due to high triplet densities. This situation may lead to singlet reformation, but such an effect is not applicable to iSF dyad systems since nongeminate triplet annihilation cannot increase with average excitation rate. Maintaining our assumption of weak chromophore coupling, we also examined possible contributions from singlet−triplet annihilation which becomes possible when a long-lived triplet resides on one of the dyad chromophores. This result showed that efficient singlet−triplet annihilation effectively nullifies the predicted large variation in fluorescence yields with excitation rates. A significant advantage of our stochastic approach is that it offers clearer views of the transition to the deterministic regime, which was accomplished here by increasing the number of chromophores. In doing so, the accuracy of predictions becomes diminished which also demonstrates why deterministic modeling of bimolecular reactions are not able predict the fine structure (i.e., multiple inflection points) observed in the ground state population as a function of excitation rate. The ability of fluorescence-based probes to serve as a qualitative indicator of iSF in isolated multichromophoric systems has important implications on further development and characterization of candidate materials. Moreover, these techniques are much more accessible than TA experiments although the latter are still essential for directly identifying singlet fission products on sub-nanosecond time scales. Last, the ability to use fluorescence opens up new opportunities for single molecule level spectroscopic studies that offer true stochastic insights of molecular photophysics as well as the influence of the local nanoenvironment.

■ ASSOCIATED CONTENT

Supporting Information

The Supporting Information is available free of charge at https://pubs.acs.org/doi/10.1021/acs.jpca.0c06966.

Further details on Monte Carlo methods, the TIPS−pentacene chromophore, and complete information on all iSF dyad kinetic models used herein (PDF)

https://dx.doi.org/10.1021/acs.jpca.0c06966
J. Phys. Chem. A XXXX, XXX, XXX−XXX

AUTHOR INFORMATION

Corresponding Author

John K. Grey − *Department of Chemistry, University of New Mexico, Albuquerque, New Mexico 87131, United States;* orcid.org/0000-0001-7307-8894; Email: jkgrey@unm.edu

Author

David J. Walwark, Jr. − *Department of Chemistry, University of New Mexico, Albuquerque, New Mexico 87131, United States*

Complete contact information is available at: https://pubs.acs.org/10.1021/acs.jpca.0c06966

Notes

The authors declare no competing financial interest.

ACKNOWLEDGMENTS

J.K.G. acknowledges financial support from the National Science Foundation (CHE-1904943).

REFERENCES

(1) Hanna, M. C.; Nozik, A. J. Solar Conversion Efficiency of Photovoltaic and Photoelectrolysis Cells with Carrier Multiplication Absorbers. *J. Appl. Phys.* **2006**, *100*, No. 074510.

(2) Smith, M. B.; Michl, J. Singlet Fission. *Chem. Rev.* **2010**, *110*, 6891−6936.

(3) Zhao, J.; Ji, S.; Guo, H. Triplet−triplet Annihilation Based Upconversion: From Triplet Sensitizers and Triplet Acceptors to Upconversion Quantum Yields. *RSC Adv.* **2011**, *1*, 937−950.

(4) Gray, V.; Dzebo, D.; Abrahamsson, M.; Albinsson, B.; Moth-Poulsen, K. Triplet−triplet Annihilation Photon-Upconversion: Towards Solar Energy Applications. *Phys. Chem. Chem. Phys.* **2014**, *16*, 10345−10352.

(5) Johnson, R. C.; Merrifield, R. E. Effects of Magnetic Fields on the Mutual Annihilation of Triplet Excitons in Anthracene Crystals. *Phys. Rev. B Condens. Matter* **1970**, *1*, 896−902.

(6) Pope, M.; Geacintov, N. E.; Vogel, F. Singlet Exciton Fission and Triplet-Triplet Exciton Fusion in Crystalline Tetracene. *Mol. Cryst.* **1969**, *6*, 83−104.

(7) Burgos, J.; Pope, M.; Swenberg, C. E.; Alfano, R. R. Heterofission in Pentacene-Doped Tetracene Single Crystals. *Phys. Status Solidi B* **1977**, *83*, 249−256.

(8) Singh, S.; Stoicheff, B. P. Double-Photon Excitation of Fluorescence in Anthracene Single Crystals. *J. Chem. Phys.* **1963**, *38*, 2032−2033.

(9) Merrifield, R. E.; Avakian, P.; Groff, R. P. Fission of Singlet Excitons into Pairs of Triplet Excitons in Tetracene Crystals. *Chem. Phys. Lett.* **1969**, *3*, 386−388.

(10) Arnold, S.; Alfano, R. R.; Pope, M.; Yu, W.; Ho, P.; Selsby, R.; Tharrats, J.; Swenberg, C. E. Triplet Exciton Caging in Two Dimensions. *J. Chem. Phys.* **1976**, *64*, 5104−5114.

(11) Arnold, S.; Alfano, R. R.; Pope, M.; Yu, W.; Ho, P.; Selsby, R.; Tharrats, J.; Swenberg, C. E. Erratum: Triplet Exciton Caging in Two Dimensions. *J. Chem. Phys.* **1979**, *70*, 1580−1580.

(12) Alagna, N.; Pérez Lustres, J. L.; Wollscheid, N.; Luo, Q.; Han, J.; Dreuw, A.; Geyer, F. L.; Brosius, V.; Bunz, U. H. F.; Buckup, T.; et al. Singlet Fission in Tetraaza-TIPS-Pentacene Oligomers: From Fs Excitation to μs Triplet Decay via the Biexcitonic State. *J. Phys. Chem. B* **2019**, *123*, 10780−10793.

(13) Yablon, L. M.; Sanders, S. N.; Li, H.; Parenti, K. R.; Kumarasamy, E.; Fallon, K. J.; Hore, M. J. A.; Cacciuto, A.; Sfeir, M. Y.; Campos, L. M. Persistent Multiexcitons from Polymers with Pendent Pentacenes. *J. Am. Chem. Soc.* **2019**, *141*, 9564−9569.

(14) Pun, A. B.; Sanders, S. N.; Kumarasamy, E.; Sfeir, M. Y.; Congreve, D. N.; Campos, L. M. Triplet Harvesting from Intramolecular Singlet Fission in Polytetracene. *Adv. Mater.* **2017**, *29*, 1701416.

(15) Korovina, N. V.; Pompetti, N. F.; Johnson, J. C. Lessons from Intramolecular Singlet Fission with Covalently Bound Chromophores. *J. Chem. Phys.* **2020**, *152*, No. 040904.

(16) Gillespie, D. T. Exact Stochastic Simulation of Coupled Chemical Reactions. *J. Phys. Chem.* **1977**, *81*, 2340−2361.

(17) Kurtz, T. G. The Relationship between Stochastic and Deterministic Models for Chemical Reactions. *J. Chem. Phys.* **1972**, *57*, 2976−2978.

(18) Srivastava, R.; You, L.; Summers, J.; Yin, J. Stochastic vs. Deterministic Modeling of Intracellular Viral Kinetics. *J. Theor. Biol.* **2002**, *218*, 309−321.

(19) Schaberle, F. A.; Serpa, C.; Arnaut, L. G.; Ward, A. D.; Karlsson, J. K. G.; Atahan, A.; Harriman, A. The Photophysical Properties of Triisopropylsilyl-ethynylpentacene—A Molecule with an Unusually Large Singlet-Triplet Energy Gap—In Solution and Solid Phases. *Chemistry* **2020**, *2*, 545−564.

(20) Gillespie, D. T. Deterministic Limit of Stochastic Chemical Kinetics. *J. Phys. Chem. B* **2009**, *113*, 1640−1644.

(21) van Stokkum, I. H. M.; Larsen, D. S.; van Grondelle, R. Global and Target Analysis of Time-Resolved Spectra. *Biochim. Biophys. Acta, Bioenerg.* **2004**, *1657*, 82−104.

(22) Chabr, M.; Wild, U. P.; Fünfschilling, J.; Zschokke-Gränacher, I. Quantum Beats of Prompt Fluorescence in Tetracene Crystals. *Chem. Phys.* **1981**, *57*, 425−430.

(23) Burdett, J. J.; Bardeen, C. J. Quantum Beats in Crystalline Tetracene Delayed Fluorescence due to Triplet Pair Coherences Produced by Direct Singlet Fission. *J. Am. Chem. Soc.* **2012**, *134*, 8597−8607.

(24) Wang, Z.; Zhang, C.; Wang, R.; Wang, G.; Wang, X.; Xiao, M. Weakly Coupled Triplet Pair States Probed by Quantum Beating in Delayed Fluorescence in Tetracene Crystals. *J. Chem. Phys.* **2019**, *151*, 134309.

(25) Funfschilling, J.; Zschokke-Granacher, I.; Canonica, S.; Wild, U. P. Quantum Beats in the Fluorescence Decay of Tetracene Crystals. *Helv. Phys. Acta* **1985**, *58*, 347−354.

(26) Lukman, S.; Richter, J. M.; Yang, L.; Hu, P.; Wu, J.; Greenham, N. C.; Musser, A. J. Efficient Singlet Fission and Triplet-Pair Emission in a Family of Zethrene Diradicaloids. *J. Am. Chem. Soc.* **2017**, *139*, 18376−18385.

(27) Pope, M.; Swenberg, C. E. *Electronic Processes in Organic Crystals and Polymers*; Oxford University Press: 1999.

(28) Bayliss, S. L.; Weiss, L. R.; Mitioglu, A.; Galkowski, K.; Yang, Z.; Yunusova, K.; Surrente, A.; Thorley, K. J.; Behrends, J.; Bittl, R.; et al. Site-Selective Measurement of Coupled Spin Pairs in an Organic Semiconductor. *Proc. Natl. Acad. Sci. U. S. A.* **2018**, *115*, 5077−5082.

(29) Ern, V.; Saint-Clair, J. L.; Schott, M.; Delacote, G. Effects of Exciton Interactions on the Fluorescence Yield of Crystalline Tetracene. *Chem. Phys. Lett.* **1971**, *10*, 287−290.

(30) Müller, A. M.; Avlasevich, Y. S.; Müllen, K.; Bardeen, C. J. Evidence for Exciton Fission and Fusion in a Covalently Linked Tetracene Dyad. *Chem. Phys. Lett.* **2006**, *421*, 518−522.

(31) de Vries, H.; Wiersma, D. A. Fluorescence Transient and Optical Free Induction Decay Spectroscopy of Pentacene in Mixed Crystals at 2 K. Determination of Intersystem Crossing and Internal Conversion Rates. *J. Chem. Phys.* **1979**, *70*, 5807−5822.

(32) Gibson, M. A.; Bruck, J. Efficient Exact Stochastic Simulation of Chemical Systems with Many Species and Many Channels. *J. Phys. Chem. A* **2000**, *104*, 1876−1889.

(33) Anderson, D. F. A Modified next Reaction Method for Simulating Chemical Systems with Time Dependent Propensities and Delays. *J. Chem. Phys.* **2007**, *127*, 214107.

(34) Lewis, P. A. W.; Shedler, G. S. Simulation of Nonhomogeneous Poisson Processes by Thinning. *Nav. Res. Logist.* **1979**, *26*, 403−413.

(35) Matsui, Y.; Kawaoka, S.; Nagashima, H.; Nakagawa, T.; Okamura, N.; Ogaki, T.; Ohta, E.; Akimoto, S.; Sato-Tomita, A.; Yagi, S.; et al. Exergonic Intramolecular Singlet Fission of an Adamantane-Linked Tetracene Dyad via Twin Quintet Multiexcitons. *J. Phys. Chem. C* **2019**, *123*, 18813−18823.

(36) Karlsson, J. K. G.; Atahan, A.; Harriman, A.; Tojo, S.; Fujitsuka, M.; Majima, T. Pulse Radiolysis of TIPS-Pentacene and a Fluorene-Bridged Bis (pentacene): Evidence for Intramolecular Singlet-Exciton Fission. *J. Phys. Chem. Lett.* **2018**, *9*, 3934−3938.
(37) Walker, B. J.; Musser, A. J.; Beljonne, D.; Friend, R. H. Singlet Exciton Fission in Solution. *Nat. Chem.* **2013**, *5*, 1019−1024.
(38) Sakai, H.; Inaya, R.; Nagashima, H.; Nakamura, S.; Kobori, Y.; Tkachenko, N. V.; Hasobe, T. Multiexciton Dynamics Depending on Intramolecular Orientations in Pentacene Dyads: Recombination and Dissociation of Correlated Triplet Pairs. *J. Phys. Chem. Lett.* **2018**, *9*, 3354−3360.
(39) Grieco, C.; Kennehan, E. R.; Kim, H.; Pensack, R. D.; Brigeman, A. N.; Rimshaw, A.; Payne, M. M.; Anthony, J. E.; Giebink, N. C.; Scholes, G. D.; et al. Direct Observation of Correlated Triplet Pair Dynamics during Singlet Fission Using Ultrafast Mid-IR Spectroscopy. *J. Phys. Chem. C* **2018**, *122*, 2012−2022.
(40) Ramanan, C.; Smeigh, A. L.; Anthony, J. E.; Marks, T. J.; Wasielewski, M. R. Competition between Singlet Fission and Charge Separation in Solution-Processed Blend Films of 6,13-Bis-(triisopropylsilylethynyl)pentacene with Sterically-Encumbered Perylene-3,4:9,10-Bis(dicarboximide)s. *J. Am. Chem. Soc.* **2012**, *134*, 386−397.
(41) Abu-Sen, L.; Morrison, J. J.; Horn, A. B.; Yeates, S. G. Concentration-and Solvent-Dependent Photochemical Instability of 6, 13-Bis (triisopropysilylethynyl) Pentacene. *Adv. Opt. Mater.* **2014**, *2*, 636−640.
(42) Lang, E.; Würthner, F.; Köhler, J. Photophysical Properties of a Tetraphenoxy-Substituted Perylene Bisimide Derivative Characterized by Single-Molecule Spectroscopy. *ChemPhysChem* **2005**, *6*, 935−941.
(43) Ambrose, W. P.; Basché, T.; Moerner, W. E. Detection and Spectroscopy of Single Pentacene Molecules in a P-terphenyl Crystal by Means of Fluorescence Excitation. *J. Chem. Phys.* **1991**, *95*, 7150−7163.
(44) Gregor, I.; Patra, D.; Enderlein, J. Optical Saturation in Fluorescence Correlation Spectroscopy under Continuous-Wave and Pulsed Excitation. *ChemPhysChem* **2005**, *6*, 164−170.
(45) Sahoo, D.; Tian, Y.; Sforazzini, G.; Anderson, H. L.; Scheblykin, I. G. Photo-Induced Fluorescence Quenching in Conjugated Polymers Dispersed in Solid Matrices at Low Concentration. *J. Mater. Chem. C* **2014**, *2*, 6601−6608.
(46) Basel, B. S.; Zirzlmeier, J.; Hetzer, C.; Phelan, B. T.; Krzyaniak, M. D.; Reddy, S. R.; Coto, P. B.; Horwitz, N. E.; Young, R. M.; White, F. J.; et al. Unified Model for Singlet Fission within a Non-Conjugated Covalent Pentacene Dyad. *Nat. Commun.* **2017**, *8*, 15171.
(47) Matsui, Y.; Kawaoka, S.; Nagashima, H.; Nakagawa, T.; Okamura, N.; Ogaki, T.; Ohta, E.; Akimoto, S.; Yagi, S.; Kobori, Y. Long-Lived Triplet Excitons Formed by Exergonic Intramolecular Singlet Fission of an Adamantane-Linked Tetracene Dyad. *ChemRxiv* **2019**, DOI: 10.26434/chemrxiv.7808435.v1.
(48) Papadopoulos, I.; Zirzlmeier, J.; Hetzer, C.; Bae, Y. J.; Krzyaniak, M. D.; Wasielewski, M. R.; Clark, T.; Tykwinski, R. R.; Guldi, D. M. Varying the Interpentacene Electronic Coupling to Tune Singlet Fission. *J. Am. Chem. Soc.* **2019**, *141*, 6191−6203.
(49) Mauch, S.; Stalzer, M. Efficient Formulations for Exact Stochastic Simulation of Chemical Systems. *IEEE/ACM Trans. Comput. Biol. Bioinf.* **2011**, *8*, 27−35.
(50) Kolomeisky, A. B.; Feng, X.; Krylov, A. I. A Simple Kinetic Model for Singlet Fission: A Role of Electronic and Entropic Contributions to Macroscopic Rates. *J. Phys. Chem. C* **2014**, *118*, 5188−5195.
(51) Sanders, S. N.; Kumarasamy, E.; Pun, A. B.; Steigerwald, M. L.; Sfeir, M. Y.; Campos, L. M. Singlet Fission in Polypentacene. *Chem.* **2016**, *1*, 505−511.

https://dx.doi.org/10.1021/acs.jpca.0c06966
J. Phys. Chem. A XXXX, XXX, XXX−XXX